ELSEVIER

Chemical Physics 205 (1996) 127–141

Chemical Physics

Competing nonradiative channels for hot electron induced surface photochemistry

M. Aeschlimann *, M. Bauer, S. Pawlik

Laboratory for Technical Chemistry, ETH Zurich, CH-8092 Zurich, Switzerland

Received 31 May 1995

Abstract

We report experiments in which we investigated the ultrafast dynamics of competing nonradiative channels for hot electron mechanisms in various polycrystalline metal samples. Time resolved two-photon photoemission, based on the equal pulse correlation technique, is used to measure the energy relaxation and the transport of the photoexcited carriers. In these studies the role of coherent effects in auto- and crosscorrelation experiments has been considered. While the inelastic lifetime of Ag is in qualitative and quantitative agreement with the Fermi liquid theory, the result obtained for Au is very different. The measured inelastic relaxation time for transition metals with unoccupied d orbitals is shorter as compared to the noble metals. The results demonstrate the feasibility of studying electron relaxation in noble and transition metals directly in the time domain and provide a framework for understanding the dynamics of hot electron transfer from a metal surface to the adsorbate.

1. Introduction

Many photoinduced reactions between adsorbed species and metal surfaces are induced by hot carriers rather than by thermal activation [1]. A possible mechanism is that photoexcited electrons in the substrate tunnel through the surface and become attached to the adsorbed molecules to form a temporary, negative molecular ion (hot electron mechanism). The hot electron is inelastically scattered back into an unoccupied electronic state of the metal substrate, leaving the adsorption system excited with some energy. If the electron spends enough time in the resonance, the excited molecule can acquire sufficient energy to desorb or to overcome the energy barrier to break some chemical bonds. One can, therefore, regard negative ion formation as the initiator of a variety of photon-stimulated surface dynamical processes.

The fundamental properties for electron-stimulated surface dynamical processes can be classified as: (a) the number of available hot electrons, (b) the total elastic and inelastic cross sections for resonance scattering by the adsorbate, (c) the competing nonradiative channels for hot electron mechanisms, and (d) the properties of the molecular resonant states on surfaces such as the lifetime of the negative ion (resonance lifetime τ_R) and the resonance potential energy surface.

Despite many challenges, the past few years have witnessed notable progress in the study of hot electron induced surface reactions in the subpicosecond time scale [1]. Stimulated by recent femtosecond laser induced desorption results, several theoretical investigations of hot carrier induced reactions have been undertaken.

* Corresponding author.

SSDI 0301-0104(95)00372-X

Gadzuk and coworkers have performed semiclassical wavepacket calculations on potential energy surfaces (PES) for hot electron induced desorption of NO on a Pt(111) surface (DIET model), calculating the desorption yield as a function of the resonance lifetime τ_R [2]. In a recent paper, Harris and Holloway calculated the desorption yield as a function of the resonance lifetime and the magnitude of the electronic barrier separating the ionized molecule (NO^-) from the Pt surface [3]. They used the same semiclassical wavepacket calculation on potential energy surfaces as Gadzuk, but treat the electron and nuclear coordinates on a equal footing. Including the connection between the potentials and the resonance lifetime enables them to describe explicitly the important electron dynamics of such processes.

Another theoretical treatment of the adsorbate response to optically induced surface uransients has been explored at IBM [4]. Stimulated by their femtosecond laser desorption results, a model has been developed to address desorption induced by multiple electronic transitions (DIMET). The distinctive feature of a femtosecond excitation is that the transition rate to the excited potential surfaces can be sufficiently high to provide multiple excitations on a time scale which is short compared with vibrational relaxation in the ground electronic state. Under such conditions, the adsorbate can accumulate the energy necessary for desorption in a series of excitation–de-excitation cycles. The model is capable of describing both the highly nonthermal regime of conventional DIET processes and the pseudothermal regime in which the molecule–surface vibration is in equilibrium with the hot substrate electronic temperature.

It is clearly understandable that, in the hot electron mechanism, the all-important factor is the lifetime τ_R of the molecule in the intermediate excited state after a charge transfer until the electron tunnels back to the metal surface. The acquired energy of the ionized molecule is directly related to the residence time τ_R. The longer the τ_R, the more kinetic energy can be acquired by the ionized molecule. Unfortunately, breaking the molecular symmetry by the substrate and the strong coupling between adsorbate excited states and electron–hole pairs of the substrate have the physical consequence of shortening the resonance lifetime τ_R to a few femtoseconds. One might expect that an increase in the barrier width would lead to an increase in the desorption probability because longer lifetimes ensure that the molecule can acquire sufficient energy to desorb before the electron tunnels back. However, according to Harris [3], there is a competing factor, because the elastic scattering probability for the incoming electron also increases with barrier width. This is due to the fact that it becomes increasingly difficult for the incident wavepacket to tunnel through the broader barrier into the molecular resonance. In other words, a wider barrier leads to greater desorption, because the lifetime τ increases and thus the molecule acquires more kinetic energy. At greater widths, however, it becomes increasingly difficult to enter the molecular resonance. On the contrary, a narrow barrier lets most electrons enter the resonance, but because the residence time is short, the molecule cannot acquire sufficient energy to desorb or to overcome the energy barrier to break any chemical bonds.

Unfortunately, neither the lifetime τ_R nor the resonance potential energy surface are known accurately from experimental observation. Both are necessary to describe the dynamics of the hot electron mechanism and would help to distinguish between the different theoretical models for ultrafast energy transfers between a metal surface and adsorbed molecules. At present, no time domain studies have successfully measured the lifetime of the molecule in the intermediate excited state. One of the authors (MA) has attempted such an experiment while at the University of Rochester [5]. No broadening of the pump–probe curve due to the resonance lifetime by the adsorption of CO on a Cu(100) surface was observed within the temporal resolution of the equal pulse correlation 2PPE technique as described in Ref. [6]. This result indicates that either the lifetime of the CO $2\pi^*$ resonance is shorter than the current detection limit (< 15 fs), or the rate of charge transfers is not high enough to produce a broadening of the autocorrelation curve. Using a similar time resolved two-photon photoemission setup to measure the resonance lifetime of CO on Cu(111), Knoesel et al. were also unable to fully time resolve the lifetime of the CO $2\pi^*$ level [7]. Within the accuracy of their data, they deduce an upper limit of $\tau_R < 20$ fs, whereas from the spectral width of the $2\pi^*$ resonance a lower limit of ~ 1 fs is estimated.

As mentioned above, next to the resonance lifetime τ_R, the cross section as well as the competing nonradiative channels for a hot electron transfer are further important factors for electron-induced surface dynamical processes. Rous has demonstrated in theory that the substrate electronic structure plays a critical role in determining the cross sections of negative ion formation at surfaces, based upon a recently developed layer Korringa–Kohn–Rostoker (KKR) calculation of resonance formation in adsorbed molecules [8]. Since for metals photoexcitation generates electrons with a distribution of kinetic energies, sharp enhancement of the electron charge transfer cross sections may not be resolved directly in a hot electron experiment. The results, obtained by Rous, however, would predict a striking enhancement of the cross section due, for example, to the coupling of the molecular resonance to the image states of the substrate.

The competing nonradiative channels for a hot electron transfer between a metal surface and adsorbed molecules are the energetic relaxation of the excited electrons and the diffusion of the excited electrons away from the surface into the bulk (transport). Both channels rapidly reduce the number of excited electrons in the surface and subsurface region which would otherwise be available for hot electron charge transfers to form a transient negative ion.

In this paper we discuss the dynamics of these two competing nonradiative channels for hot electron charge transfers. We perform time resolved two-photon photoemission, based on the equal pulse correlation technique, to investigate systematically these competing channels at different polycrystalline metal surfaces. In particular, we show that the study of the ultrafast dynamics of optically excited carriers in metals can provide valuable information on the role of the various interaction mechanisms for the relaxation and thermalization process.

2. Time resolved two-photon photoemission technique (2PPE)

The experimental determination of the properties of the unoccupied electronic states on clean and adsorbate covered metal surfaces, which normally play an important role in chemical reactions, has been made possible by the development of inverse photoemission [9] and two-photon photoemission (2PPE) [10]. Two-photon photoemission currently permits measurements to be made with relatively high resolution (as an example, see Ref. [11]). In a 2PPE experiment two excitation steps occur. In the first step electrons from occupied states at or below the Fermi level E_F are excited to normally unoccupied states with energies between the Fermi and vacuum levels. The second step is photoionization of the transient population from the excited level and detection of the photoelectron by an energy analyzer. Hence, in two-photon photoemission from solids the photon energy must not exceed the work function, and the intermediate states are limited to the range between E_F and E_{vac}.

Combined with ultrafast laser techniques, time resolved 2PPE is one of only few techniques that can monitor the state of the adlayer and substrate during the course of the transformation by laser induced surface reactions. This is made possible by the fact that it is a two-photon process which is sensitive to the density and lifetime of the intermediate (unoccupied) state. The dynamic information can be obtained by means of a pump–probe experiment in which the first laser pulse pumps electrons in the intermediate state, followed by a second pulse which subsequently photoemits the excited electrons. By varying an optical delay line between the two pulses, the lifetime of the intermediate (unoccupied) states can be determined.

Our pump–probe experiments are carried out in an UHV chamber by monitoring the number of electrons at a given kinetic energy as a function of the delay between the pump and probe pulses. The two pulses, equal in energy and either parallel or crosspolarized, propagate collinearly in order to avoid effects due to the buildup of intensity or polarization gratings. We used laser pulses at low fluence and peak power to avoid space charge effects or highly excited electron distributions. Therefore, we measured the relaxation and transport of individual excited electronic states rather than the collective behavior of transiently heated nonequilibrium distribution. This is an important distinction, because much photoinduced surface chemistry is a result of the nascent (as photoexcited), nonthermal electron distri-

bution which have energies from 1 to 6 eV and not the subsequent thermally equilibrated electron distribution in which the average energies are only a few tens to hundreds of meV. That is, for example, the hot electron induced molecular processes at metal surfaces occur even before the excited electrons equilibrate among themselves.

The direct measurement of electron relaxation times in metals is challenging, because it should be performed in the few femtosecond time domain. Only recently, Schmuttenmaer et al. demonstrated the feasibility of studying the relaxation of single excited electrons at the Cu(100) surface in the time domain by means of two-photon photoemission [6]. We used the same equal pulse correlation technique to investigate systematically the hot electron energy loss lifetime not only of noble metals but also of catalytically more active transition metals. Compared with noble metals, in which the d shell is completely filled, the d band of transition metals is only partially filled, and the electronic and relaxation properties are dominated by these d electrons to a considerable degree. The strong localization of these d electrons results in a narrower band and hence in a much higher density of states near the Fermi level as compared with the s–p electrons. A higher density of occupied and unoccupied states near the Fermi level is expected to lead to faster relaxation and hence to a shorter inelastic lifetime of excited electronic states.

In principle, using the energy and time resolved 2PPE technique, we measure the depletion of an excited state population in the very surface region. There are two factors which might affect the measured dynamics: cascade effects and transport of the excited carriers away from the surface region into the bulk. The population of a state may be filled due to the energetic decay of electrons at higher excited electronic state (cascade effect). In order to be certain that we are measuring the lifetime of single excited electrons and not the relaxation time of a cascade, we have to roughly calculate the fraction of excited electrons. Typically, we have a laser fluence of about 0.3 nJ/pulse in each beam resulting in 6×10^8 photons per pulse. For a spot size of ~ 150 μm and a penetration depth of the blue light of ~ 150 Å, the volume where the laser light will be absorbed is about 3×10^{-10} cm^3. If 10% of the light is absorbed by the metal, then 6×10^7 photons are absorbed by 7×10^{13} atoms which results in a fractional excitation of roughly 1 part in 10^6. Hence, there will be essentially no hot electron–hot electron scattering and therefore possible cascade effects at higher excited states are minimized. According to Quinn [12], the electron loses about half of its excitation energy in a typical collision. At a photon energy of $h\nu = 3.3$ eV, the highest excited state will be 3.3 eV above the Fermi level. For the energy range between about 2 and 3.3 eV, there is only a slight chance that the probed state may be filled again by cascade electrons, taking into account our small number of excited electrons and the large fraction of energy loss by a typical collision of the hot electron with a Fermi electron. Below 2 eV, the depletion of an energetic population might be influenced by the cascade electrons, but the increase of the specific lifetime due to cascade effects cannot be larger than the relaxation of the higher energetic states where the electron originates. As seen, for example, in Fig. 7, the relaxation time of excited states above 3 eV is shorter than 2 fs and hence shorter than the time resolution of our setup. Below 1 eV, however, cascade effects will definitely start to play an important role for electron relaxation measurements.

The second factor which influences the 2PPE measurement of the electron dynamics is the transport of the photoexcited electrons away from the surface region. This will reduce the photoelectron intensity near the surface region emitted by the probe pulse and will set a lower limit for the measurement of the lifetime by 2PPE. For example, even if the electrons had an infinitely long lifetime, there would still be an experimentally measured decay in the photoelectron yield as a function of pump–probe delay time due to the electron moving away from the surface and out of the probe volume. If we assume separate mechanism for decay and transport we can add up the measured decay rate in accordance with Matthiessen's rule:

$$\frac{1}{\tau(\text{measured})} = \frac{1}{\tau(\text{transport})} + \frac{1}{\tau(\text{intr. decay})} \tag{1}$$

leading to $\tau(\text{measured}) < \tau(\text{transport})$. Hence, the decay of the single excited electronic state as a function of the time delay between the two pulses

depends on the same parameter as the competing channels for hot electron mechanisms: intrinsic decay of the excited energetic state and transport. Unfortunately, it is not easy to study either the decay or the transport effect independently of each other. For example, a change in the film thickness can influence the transport of the electrons as well as the inelastic lifetime of the electrons.

Finally, at energies very close to the Fermi level where the inelastic lifetime increases beyond 30 fs, electron–phonon scattering becomes important. However, phonon energies are only a few meV for typical metals. Hence the energy loss due to phonon creation is too small to be resolved by our energy analyzer. Therefore, even when the excited electron lost some energy due to the creation of a phonon, it still will appear in our energy analyzer. Electron–phonon scattering, however, destroys the phase information of the electrons, causing a weaker coherent contribution to the 2PPE signal for a parallel polarized setup. As discussed under polarization effects, this will reduce τ(pp).

3. Experimental setup

A schematic overview of the experimental setup is shown in Fig. 1. The samples are mounted in a UHV chamber equipped with a cylindrical sector analyzer. In general, we use a pass energy of either 4 or 8 eV, leading to 50 or 100 meV resolution respectively. Before the experiments, the sample surface was carefully cleaned by argon ion sputtering and annealing cycles. The cleanliness was routinely checked with Auger electron spectroscopy (AES). The sample was kept at room temperature unless stated otherwise.

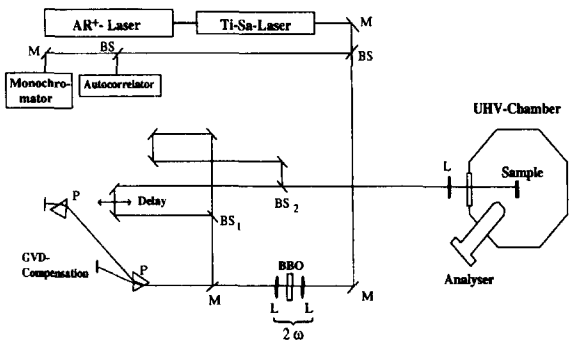

Fig. 1. Schematic diagram of the equal pulse correlation setup for time resolved 2PPE. The output of a mode-locked Ti:sapphire laser is frequency doubled (2ω) and external prisms precompensate for group velocity dispersion (GVD). After splitting by a beamsplitter (BS_1) the resulting pulses are delayed with respect to each other. A second beamsplitter (BS_2) combines both pulses collinearly, which are then focused onto the sample in a UHV chamber.

The time resolved 2PPE experiments were performed with a femtosecond mode-locked Ti:sapphire laser, pumped by about 8 W from a cw Ar^+ laser. The system delivers transform-limited and $sech^2$ temporal shaped pulses of up to 9 nJ/pulse with a duration of 40 to 50 fs at a repetition rate of 82 MHz and a tunability from 730 to 830 nm. The linearly polarized output of the Ti:sapphire laser is frequency doubled in a 0.2 mm thick beta barium borate (BBO) crystal to produce UV pulses at $h\nu = 3$ to 3.4 eV. The UV beam is sent through a pair of fused silica prisms to precompensate for pulse broadening due to dispersive elements like lenses, beamsplitters and the UHV chamber window in the optical path. A GVD and intensity loss matched interferometric autocorrelator setup was used for the pump–probe experiment. The pulses are split by a beamsplitter in equal intensity (pump and probe pulses), and one path is delayed with respect to the other by a computer controlled delay stage. Both beams are combined collinearly – either parallel or crosspolarized – by a second beamsplitter and are focused through a fused silica lens ($f = 200$ mm) at the sample surface. The beams enter the UHV chamber through a suprasil viewport.

By using a low pulse energy (< 0.3 nJ/pulse) and a high repetition rate laser, we avoid space-charge effects that can distort the measured photoelectron spectrum. The count rate is much less than one electron per pulse. Assuming a spot size of ~ 150 μm we estimate a pulse fluence of typically 1.5 $\mu J/cm^2$ at the sample surface under these conditions (temporal and spatial overlap).

If not otherwise stated, the linearly polarized laser beam is incident perpendicular to the sample surface in order to avoid problems regarding the different absorption efficiency of p- and s-polarized light. In addition, perpendicular incidence avoids coupling of the light into surface plasmons [13] which can influ-

ence the relaxation results quite drastically. The entrance axis of the energy analyzer is 45° with respect to the laser beam. A −4.0 V bias is applied to the sample to eliminate the effects of any stray electric fields.

A typical two-photon photoemission spectrum of a polycrystalline gold foil, taken with one of the beams blocked, is shown in Fig. 2. The spectrum is determined by the electronic band structure, the photon energy, and the lifetime of the intermediate state. A longer lifetime increases the cross section for the absorption of a second photon.

As seen in the inset, the energy of the intermediate state E_i above the Fermi energy E_F is given by

$$\varepsilon = E_i - E_F = \Phi + E_{Kin} - h\nu, \qquad (2)$$

where E_{Kin} is the detected electron kinetic energy at the sample surface (bias voltage already subtracted), and $h\nu$ is the photon energy. Because the lifetime of the intermediate state increases rapidly with the decrease in excitation energy, as shown below, the 2PPE yield will increase at lower kinetic energy even for flat bands like the Ag or Au s–p bands.

The pump–probe experiments are carried out by monitoring the number of electrons at a given kinetic energy as a function of delay between the pump and probe pulses (two-pulse correlation experiment). Scans obtained when monitoring electrons at 0.1 and 1.3 eV of kinetic energy (1.8 and 3 eV above the Fermi level respectively) are shown in Fig. 3. An

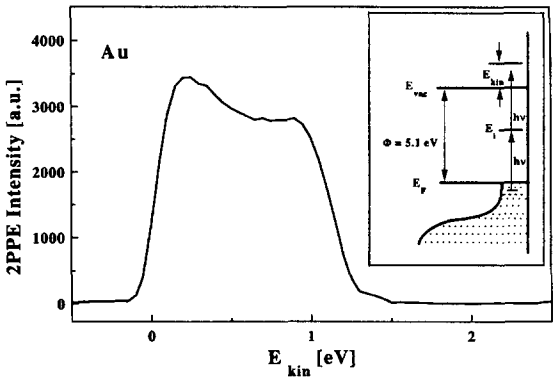

Fig. 2. 2PPE spectrum of a clean polycrystalline gold surface obtained with p-polarized light at $h\nu = 3.2$ eV. The inset shows a schematic figure of the two-photon process where Φ is the work function for the sample, E_i is the intermediate state, E_{vac} is the vacuum level and E_F is the Fermi level.

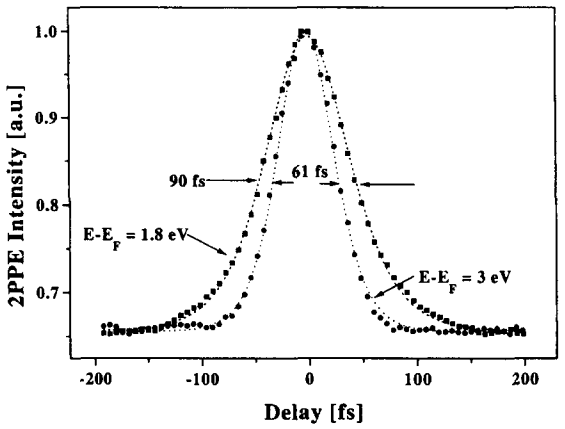

Fig. 3. 2PPE autocorrelation traces obtained from a polycrystalline gold film. The energy difference $E - E_F$ indicates the intermediate state energy in the two-photon photoemission process and not the kinetic energy of the emitted electrons. The dashed lines represent a fit to a sech^2 function with full width at half maximum (fwhm) of 90 and 61 fs.

experimental effect on the signal is caused by the finite pulse width of our probe. Therefore, two-pulse correlation data are, in fact, the results of the convolution of the actual signal (decay function) with the pump and probe pulse. By deconvoluting the decay function from the laser pulse autocorrelation curve, we can obtain the lifetime τ(measured) of the intermediate state. The main difficulty, however, is to find the electric field autocorrelation curve for the laser pulse in the UHV chamber (underlying instrument response function), because we are not able to autocorrelate the frequency doubled output of the laser system (360–410 nm) with a doubling crystal to determine its fwhm. However it is expected and has been proven by our experiments, that for transition metals with a large amount of unoccupied d orbitals, the inelastic lifetime τ is shorter than 2 fs at higher excitation energies ($E - E_F > 3$ eV). Electrons at those energies relax faster than we can observe within our time resolution. Hence, the fwhm of the two-pulse correlation signal decreases to a nearly constant value at higher energies and this value is within < 2 fs consistent with the electric field autocorrelation curve of the laser pulse. Therefore we rely on the two-pulse correlation spectra of Ta and Rh at the highest electron kinetic energies to determine the underlying instrument response function.

We used a nonlinear least-squares fitting routine to deconvolute the exponential component of the correlation trace. For small values of τ compared to the laser pulse width, however, a numerical deconvolution to obtain τ becomes complicated. The most important aspect of our investigation is the relative trend of τ versus energy for different metals and not the absolute value of τ. Therefore, as a first approximation, we compared the fwhm of our measured correlation curve with a calibration curve fwhm versus τ. This calibration curve was numerically obtained by the convolution of the actual instrument response function with a exponential decay function, using τ as the variable.

Furthermore, Fig. 3 shows how a subpulse resolution of only a few fs can be obtained by using the equal pulse crosscorrelation technique. In spite that the fwhm of the crosscorrelation curve is about 60 fs (fwhm of the laser pulse = 39 fs) we are able to determine a change in the fwhm of only one or two fs, as long as the laser pulse width, averaged over 10^8 pulses, is sufficiently stable. With our set up, the correlation trace fwhm is stable within ~ 2 fs on a timescale of a few hours.

Unfortunately, the finite wavelength tunability (720 to 830 nm) of the Ti : sapphire laser limits our ability to measure the inelastic relaxation of states very close to the Fermi level. For instance, the deepest level we are able to probe is the work function Φ of the material minus the photon energy $h\nu$. Further experiments are being undertaken to probe levels closer to the Fermi energy by lowering the work function due to Cs adsorption and will be published elsewhere [14]. Since the alkali adsorption introduces new surface states, which might be resonant with the intrinsic electronic states, these conditions can change the electronic relaxation processes on the surface by introducing new relaxation or quenching channels.

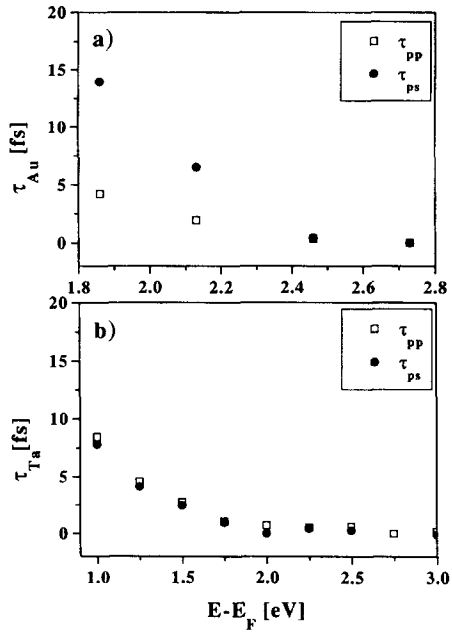

Fig. 4. Relaxation time constants τ as a function of the intermediate state energy $E - E_F$ for gold (a) and tantalum (b). The filled circles represent the results of crosscorrelation a measurement (τ_{ps}) and the open squares of an autocorrelation measurement (τ_{pp}). Note the strong polarization dependent lifetime difference $\Delta = (\tau_{ps}) - (\tau_{pp})$ for Au whereas no difference was observed for Ta.

4. Polarization effects

First we briefly comment on the nature of polarization effects observed in our experiments. Fig. 4a) shows the energy-dependent relaxation time τ(measured), for a polycrystalline gold foil, using parallel polarized pulses (pp) as well as crosspolarized pulses (ps). τ has been deconvoluted from the experimental data as a function of intermediate state energy $\varepsilon = E_i - E_F$. We did not find a difference in τ between (pp) and (ss) measurements within our time resolution. The observed difference between τ(pp) and τ(ps) may be astonishingly large but can be explained by the different ratio between coherent and noncoherent two-photon photoemission in the signal. The light of an ultrashort laser pulse has in general a strong degree of coherence and therefore introduces coherence in the carrier system [15]. If the physical phenomena under investigation occur on a time scale shorter than the dephasing time T_2, such as the interaction of the carriers with the external light field in order to accept a second photon, coherent effect cannot be separated and has to be taken into account [16]. This experiment proves that, due to the typical time scale of the lifetime of excited carriers, coherent phenomena become very important in energy relax-

ation experiments. The dephasing process is a quasi-elastic process in which phase breaking scattering events destroy the phase coherence of the electrons but do not remove the electrons from the quantum state of interest. The coherent part is the convolution between the dephasing function and the electric field autocorrelation and is, therefore, not an instantaneous (or just virtual) response of the medium. For an exact theoretical analysis of coherent phenomena in 2PPE, a fully quantum-mechanical treatment is required. However this would go beyond the scope of this paper.

When the two pulses are orthogonally polarized and propagate collinearly in the same direction, the coherent effect is drastically reduced, resulting in a nearly sequential (noncoherent) two-photon process. Although there might be some small coherent contributions, the measured lifetime of the ps (orthogonal polarized) measurement can be regarded as the relaxation of the excited energetic state near the surface. However, the role of coherence effects in the interpretation of data gained by subpulse resolution techniques must be borne in mind in order to correctly extract the energy relaxation time T_1. By investigating the difference between τ(pp) and τ(ps), we are able to discuss the dynamics of the coherent polarization in the carrier system and its decay by pulse relaxation. The coherent polarization decays within a period of time that is typically much shorter than that related to incoherent phenomena, leading to $T_2 < T_1$, where T_1 is the inelastic energy relaxation time of the excited electron. For a noble metal with a long T_1, the dephasing time T_2 can become much shorter than T_1. Because only τ(pp) is strongly influenced by T_2, $\tau(\mathrm{pp}) < \tau(\mathrm{ps})$ as seen in Fig. 4a for polycrystalline gold. After several additional sputter and annealing cycles of the gold foil, we observed very little change for τ(ps); however, τ(pp) increases resulting in a decreasing difference $\Delta = \tau(\mathrm{ps}) - \tau(\mathrm{pp})$. This behavior can be explained by the fact that cleaning and annealing processes reduce elastic carrier impurity and carrier defect scattering, causing an increasing dephasing time T_2.

Furthermore, we investigated the polarization dependent lifetime difference $\Delta = \tau(\mathrm{ps}) - \tau(\mathrm{pp})$ for transition metals with a very short inelastic energy relaxation time T_1. The dephasing time T_2 will be limited by inelastic electron–electron scattering processes and therefore by T_1, leading to equal τ(pp) and τ(ps) as seen for tantalum in Fig. 4b.

5. Inelastic lifetime of single excited electrons

For optical radiation in the visible wavelength regions, the photons are absorbed by the creation of carriers, i.e., through the production of electron–hole pairs. Initially these carriers are far from being in equilibrium with the temperature of the substrate. The lifetime of the electronic excitation will be controlled by the available decay channels, which generally include collisions with other electrons and phonons. Hot electron energy loss lifetime in metals have been the focus of research for many years. A knowledge of this process is important from the point of view of basic physics, such as electron–electron and electron–phonon scattering. There are related problems, such as the probing depth of low energy electrons by different surface sensitive analytical techniques.

In principle, lifetime of carriers can be obtained in the time as well as in the frequency domain. Before it was possible to use ultrafast lasers for real time experiments, the only means available for obtaining information about lifetimes of states was the measurement of spectroscopic linewidth. This method, however, is controversial, because experimental results have proven that lifetime is not necessarily the primary factor in the observed linewidth of unoccupied states even at simple metal surfaces (as an overview, see Ref. [17]). Kevan demonstrated by means of high resolution angle-resolved photoemission spectroscopy on the sp surface state on Cu(111) that the spectral width of the feature even shows a counter intuitive behavior, i.e., the width actually increased upon approaching the Fermi level [18]. In addition, it is quite obvious that it will be impossible to determine the relaxation rate of polycrystalline metals from frequency domain measurements because, in general, no discrete spectral features exist.

At present, the ultrafast dynamics of optically excited carriers have been studied quite intensively for semiconductors. Time domain studies have provided valuable information on the role of the various interaction mechanisms for the thermalization and relaxation process [19]. Due to the existence of a

band gap, the electrons will initially cool to the bottom of the conduction band, and the holes will cool to the top of the valence band. At high carrier densities, carrier–carrier scattering is the dominant thermalization process; at low densities the interaction with optical phonons is the dominant mechanism leading to the formation of phonon replicas in the carrier distribution function. The resulting lifetimes of the thermalized excitations vary widely and can extend into the nanosecond range.

In the case of metals without a restriction of unoccupied orbitals due to a band gap, the hot electrons relax directly to a thermal equilibrium with the whole electron gas. Therefore, the lifetime of individual excited electronic states is always short, typically in the order of only a few femtoseconds. In metals a detailed study of relaxation phenomena in the time domain has just begun [6,20,21]. The relaxation of a single electronic state must be separated from the much slower relaxation of a highly excited electron gas by electron–phonon scattering, where the energy is transferred from the hot electron gas to the lattice. This thermalization process has already been quite well investigated by indirect methods, such as the techniques of transient thermoreflectivity [22] and transient thermotransmissivity [23]. Both are pump–probe techniques based on the temperature dependence of the dielectric constant which, of course, depends on the collective behavior of a transiently heated nonequilibrium electron distribution.

In metals the important decay channels at low carrier density are quite different compared to semiconductors. Carrier–carrier interaction, carrier–phonon interaction, and carrier photogeneration processes play minor roles in the energy relaxation of hot electrons. Only at energies close to the Fermi level, where the inelastic lifetime increases rapidly, does electron–phonon scattering become more important. Spontaneous recombination processes (luminescence) typically occur on much longer times scales than the electron–electron and electron–phonon scattering processes. Thus, they are of minor importance for the ultrafast dynamics of photoexcited carriers.

At low laser fluence, the dominant hot electron relaxation process is inelastic scattering of the excited electrons with Fermi electrons and electrons of occupied states just below the Fermi level, leaving both electrons in unoccupied states above the Fermi level. Defects and impurities will increase the elastic scattering rate but have a smaller effect on the inelastic scattering rate. For polycrystalline samples, inelastic scattering on grain boundaries is a further source for energy relaxation of excited electrons.

The total scattering cross section is given by $\sigma(E) = 1/\lambda_i(E)$, where λ_i is the inelastic mean free path of the excited electrons and can be translated via the electron group velocity $v(E)$ into the inelastic lifetime $T_1 = \lambda_i/v(E)$. A large amount of data for λ_i has been accumulated from the overlayer method in which the attenuation of a prominent substrate feature is measured as a function of the overlayer thickness x and fitted with an exponential decay $\exp(-x/\lambda_i)$. The data for many materials are often displayed as a "universal curve" which shows λ_i as a function of energy [24]. With low energy electrons escaping from the solid close to the vacuum layer, the overlayer method cannot be applied due to the lack of a distinguishing feature. However, by depositing nonmagnetic thin layers on a magnetic surface, one can obtain accurate values of λ_i in the energy range of $5 < \varepsilon < 10$ eV, where $\varepsilon = (E_i - E_F)$, by measuring the decay of the spin polarization P of the emerging electrons. The results show, that for many metals, the values in this energy range cannot be described by the "universal curve" [24]. Siegmann has compiled the data of $\lambda_i(5 < \varepsilon < 15$ eV) available from many laboratories and has found a fairly simple behavior [25]: the total scattering cross section σ can be fitted to the data by

$$\sigma = \sigma_0 + n\sigma_d. \tag{3}$$

The constant part σ_0 accounts for inelastic scattering other than into the holes of the d band and includes, for instance, scattering into s–p-derived bands, whereas the second part σ_d describes the scattering into one unoccupied d orbital, where n is the number of unoccupied d orbitals. This empirical rule describes the strong difference of the total scattering cross section σ of different transition metals astonishingly well. According to Siegmann's interpretation, the noble metals Cu, Ag, and Au should have identical $\sigma = \sigma_0$. That this is not the case for $\varepsilon < 5$ eV will be shown below. However, as Siegmann pointed out, it is obvious that Eq. (3) cannot be

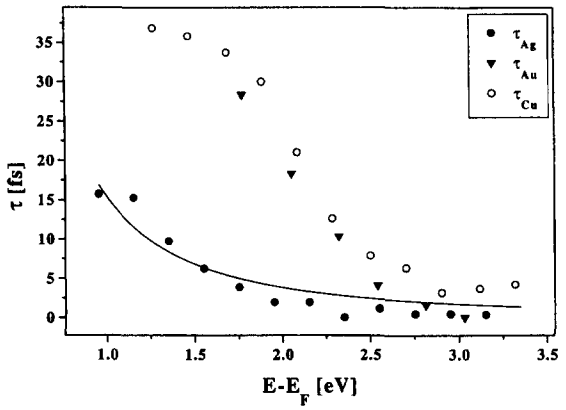

Fig. 5. Comparison of the relaxation time constants obtained from crosscorrelation measurements of different noble metals. The triangles represent the data for Au and filled circles for Ag. The open circles are the results for Cu(100) surface, published by Ref. [6]. The solid line is calculated from Fermi liquid theory.

used to describe the details of electron–electron scattering in metals. For example, it neglects the scattering into the variable surface or interface states. Furthermore, electronic changes in the substrate surface do occur when the overlayer is deposited [25].

For studying single excited electron relaxation as a competing nonradiative channel for the hot electron charge transfers, we are mainly interested in the energy range below the vacuum level which cannot be tested by the overlayer method. Time domain measurements are therefore required to determine the excited state lifetime of energies below the vacuum level.

6. Noble metals

Fig. 5 displays the inelastic lifetime $T_1 = \tau(\mathrm{ps})$ versus the energy $\varepsilon = (E_i - E_F)$ for an Au and an Ag foil. We used polycrystalline film in order to limit electron transport which is impeded by elastic electron–grain boundary collision as will be discussed below. τ(ps) varies slightly from measurement to measurement (max. ~ 15%), depending on the sample preparation (e.g. grain size, lattice imperfection, surface roughness). The lifetime τ increases as the energy of the intermediate state above the Fermi level decreases. The source of the increasing lifetime near the Fermi level is the decreasing phase space for scattering and hence a consequence of the exclusion principle on electron–electron scattering. In order for a single excited electron at the intermediate energy E_i to be scattered, it must interact with an electron of a state below E_F. The exclusion principle requires that these two electrons can only scatter into unoccupied levels whose energies must, therefore, be greater than E_F. Consequently, the lifetime of an electron at the Fermi surface at $T = 0$ is infinite. When E_i is slightly different from E_F, some phase space $|E_i - E_F|$ becomes available for the scattering process. According to the Landau theory of Fermi liquids, this leads to a scattering rate which scales like $(E_i - E_F)^2$ [12]. The square factor comes from the available independent energy variable for the e–e scattering process in a three-dimensional system. A nonzero electronic temperature provides an additional range of phase space of the order of $k_B T_e$ and therefore leads to a scattering rate going as $(k_B T_e)^2$. Taking these consideration into account, an excited electron has a scattering rate $1/\tau$ that depends on its energy and the temperature in the form [26]:

$$1/\tau = a(E_i - E_F)^2 + b(k_B T_e)^2. \quad (4)$$

We expect another increase in the phase space available for scattering due to the nascent, nonthermal electron distribution caused by the fs pump and probe laser pulses. From the fact that the number of excited electrons scales linearly with the laser fluence I_L, we add, as a crude approximation, an optical contribution cI_L^2 to the scattering rate, extending Eq. (4) to yield

$$1/\tau = a(E_i - E_F)^2 + b(k_B T_e)^2 + cI_L^2. \quad (5)$$

Inherent in the above analysis is the assumption of separate mechanisms for the temperature induced and optical induced scattering rates. This assumption is certainly violated for a longer lifetime τ. At a higher value of $\varepsilon = (E_i - E_F)$ the leading contribution to the scattering rate $1/\tau$ is the first term. Terms 2 and 3 of Eq. (5) are usually small, but at lower ε and higher laser density it may be large enough to cause an overall increase in the scattering rate.

In order to check whether τ is influenced at lower energies ε by the pump and probe pulses and hence by the probing technique itself, we determined the change in τ as a function of T_e. Fig. 6a shows the

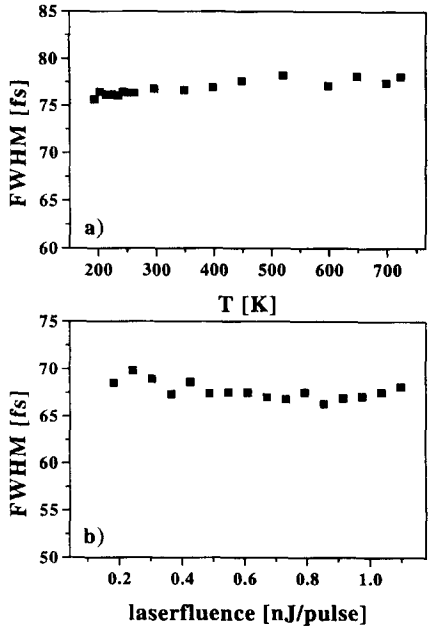

Fig. 6. fwhm of the crosscorrelation traces obtained from polycrystalline gold film as a function of temperature (a) and the laser fluence (b). $E - E_F = 1.85$ eV.

fwhm of a crosscorrelation experiment as a function of the sample temperature. We observed a slightly decreasing fwhm as the temperature is decreased from 700 to 200 K (the same slope was obtained by heating from 200 to 700 K). This is contrary to what was expected, because the scattering rate should increase with T_e. However, the change in fwhm is within the time resolution of our set up and can be regarded as a technical artifact due to the heating of the sample. According to nonequilibrium heating model calculations, the femtosecond pump and probe pulses did not cause an increase in the electron temperature by more than ~ 10 K [27]. Consequently, even when the lifetime was long enough for a partial thermalization of the electron gas, causing a minor increase in T_e, the scattering rate will not be influenced within our time resolution.

In addition, the importance of the optical contribution to the scattering rate can be investigated by varying the laser fluence I_L . In Fig. 6b we plotted the measured fwhm as a function of the laser fluence I_L. The result does also not show measurable dependence of τ caused by the (laser induced) increased phase space.

The same phenomena shown in Figs. 6a and 6b were also observed with Ag. Hence it is reasonable to expect that, under the quoted experimental conditions and uncertainties, the deviation of electron distribution, due to the pump and probe laser pulses, does not significantly affect the measured lifetime $\tau(\varepsilon)$. The dominant scattering term in the probed energy range is given by the available phase space $\varepsilon = (E_i - E_F)$.

According to Eq. (3), all noble metals should have an identical total inelastic scattering cross section $\sigma = \sigma_0$ which is obviously not the case for Au and Ag as seen in Fig. 5. A more detailed, semiquantitative description of the properties of electrons in metals with several eV of excitation energy above the Fermi level is obtained by treating the excitation as a quasiparticle and is referred to as Fermi liquid theory. Using the approach taken by Quinn [12], we can estimate the lifetime of the excited electrons by calculating the imaginary part of their self energy E_I. For low energy excitation ($k/k_F < 1.3$) the approximate electron lifetime can be given as

$$\tau = h/2E_I = a\left[E_F/(E_i - E_F)\right]^2, \qquad (6)$$

where a is a prefactor depending on the dimensionsless parameter r_s/a_0 for the interelectron spacing. The solid line in Fig. 5 corresponds to the predicted lifetime for Ag obtained from Eq. (6) with $r_s/a_0 = 3.02$ [26] leading to a prefactor $a = 0.5$ (according to Ref. [12]).

It is obvious that the data obtained for the Ag film are reasonably close to the Fermi liquid theory; the deviation for Au of the measured lifetime from the Fermi liquid theory is, however, quite remarkable. To determine whether this discrepancy is due to inelastic surface scattering of the excited electrons, caused by a different surface roughness of the Ag and Au foils, we evaporated 200 nm thick Ag and Au films on a NaCl and on a mica substrate respectively. Both films went through different cleaning and annealing cycles to improve the smoothness of the surface. However the obtained results show only minor differences to the results obtained with the foils. The discrepancy between the experimentally observed lifetime T_1 of the Ag and Au films cannot be understood in terms of the Fermi liquid theory. Both critical parameters in Eq. (6), the radius of the

sphere r_s and the Fermi energy E_F, are nearly equal for Ag and Au. In contrast to our results, Groeneveld et al. found for both metals the same prefactor $aE_F^2 = 10$ fs eV^2 according to Eq. (6), using a novel femtosecond optical transient reflection technique [21]. A related study of Schmuttenmaer et al. found, however, the same deviation of the relaxation time τ for a single crystal Cu(100) sample from Fermi liquid theory as our Au results [6]. These copper values are included in Fig. 4.

This deviation of Cu and Au from the Fermi liquid theory might be caused by the occupied d orbitals, which are located just about 2.3 eV below the Fermi level for both metals and exhibit strong non-free-electron-like behaviors. In contrast, the d orbitals of Ag are much deeper, about 4 eV below E_F. Further investigations of a possible influence of the d bands on the measured lifetimes are in progress.

7. Transition metals

We extend the relaxation studies to transition metals to examine the effect of the different band structures in the relaxation process. Fig. 7 shows the inelastic lifetime τ(ps) versus the energy $\varepsilon = (E_i - E_F)$ for a tantalum and a rhodium foil. As expected and as discussed above, the inelastic relaxation time τ for transition metals with unoccupied d orbitals is shorter compared to the noble metals. We will compare our results with Siegmann's empirical rule (3).

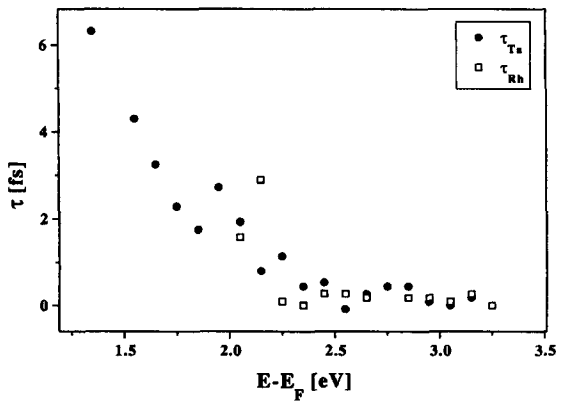

Fig. 7. Comparison of the inelastic lifetime τ obtained from crosscorrelation measurements of the transition metals tantalum (●) and rhodium (□).

The number of unoccupied d electrons is much larger for Ta ($5d^3$) than for Rh ($4d^8$), however, the measured τ(Rh) is within our time resolution equal to τ(Ta). There is a possible explanation for the observed discrepancy from Eq. (2). Siegmann has compiled the data of λ_i in the energy range of $5 < \varepsilon < 15$ eV, therefore all unoccupied d orbitals can be taken into account. Using the 2PPE technique, we investigate the inelastic lifetime of states below the vacuum energy and, therefore, have to compare the number of unoccupied d orbitals below the probed intermediate level. Although Ta has much more unoccupied d orbitals than Rh, these unoccupied orbitals are distributed over a wide energy range above the Fermi energy ($E_F < \varepsilon < E_F + 5$ eV [28]). In comparison, most of the unoccupied d levels of Rh are within the energy range into which the scattered electrons can fall.

8. Transport

The transport of excited electrons from the surface into the bulk has the same effect as the decay of the excited electrons: it reduces the number of electrons at the surface region which might otherwise transfer to the molecule. The inelastic mean free path λ_i is the product of the lifetime and the velocity. In gold, the excited electron velocity is roughly 2×10^8 cm/s at 1.9 eV above the Fermi level. Therefore, λ_i ($T_1 = 20$ fs) is roughly 400 Å at 1.9 eV. Brorson et al. have shown that hot electron transport across 500–3000 Å gold films can proceed at a velocity approaching that of the Fermi velocity [29]. These measurements provide significant evidence of a ballistic component in electronic transport. The relative magnitude of ballistic versus diffusive heat transport in gold is, however, still unresolved.

As an approximation we performed a numerical calculation of the hot electron distribution perpendicular to the surface (z-axis) as a function of time using a simple isotropic ballistic transport model. The photoexcited electrons are free to move with equal probability in all directions, and we incorporated total elastic reflection at the surface. Because the laser beam diameter is much larger than the optical skin depth, we neglect radial diffusion of the hot electrons which is negligible within the time

scale of interest. Fig. 8 displays the electron distribution at the excitation time $t_0 = 0$ fs, given by the exponential decay of the laser light absorption, and the calculated distribution at a later time $t = 30$ fs. The curves indicate the drastic reduction of excited electrons in the important surface region within 30 fs due to the transport into the bulk, thus causing a strong reduction of the cross section of a hot electron charge transfer process.

From the experimental point of view, transport also reduces the photoelectron intensity emitted by the probe pulse and will set a lower limit for the measurement of the lifetime by 2PPE. Schmuttenmaer et al. have shown for Cu(100) that the quadratic trend of the electronic lifetime predicted by the Fermi liquid theory does not continue at lower energies, and that this leveling off of the apparent lifetime can be attributed to the transport effect [30]. This leveling off starts at $\sim < 2$ eV. The work function for a clean polycrystalline gold surface is too high for this leveling off to occur. The deepest level which we are able to probe is about 2 eV. We decreased the work function slightly by depositing a small amount of Cs on the surface of the 2000 Å thick gold film and found the same leveling off effect of the apparent lifetime at energies < 1.8 eV (see (□) in Fig. 9).

Possibilities for reducing the transport effect and increasing hot electron induced molecular processes on metal surfaces were investigated. By comparing transient thermotransmissivity results of single crystalline and polycrystalline gold films, Elsayed-Ali et al. have shown that electron transport is impeded by the predominantly elastic electron–grain boundary collision [27]. Grain boundaries are known to be very efficient in scattering excited electrons.

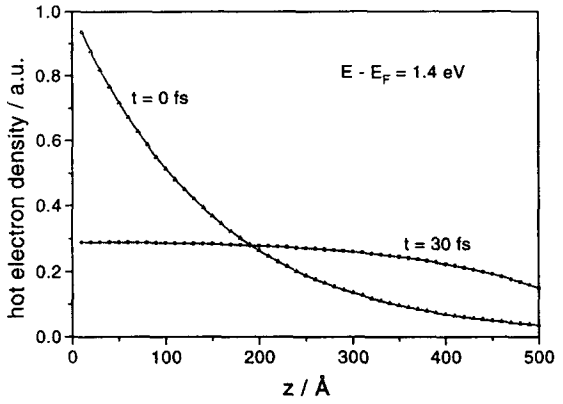

Fig. 8. Excited electron distribution perpendicular to the surface (z-axis) at the excitation time t_0 and after 30 fs as predicted by an isotropic ballistic transport model.

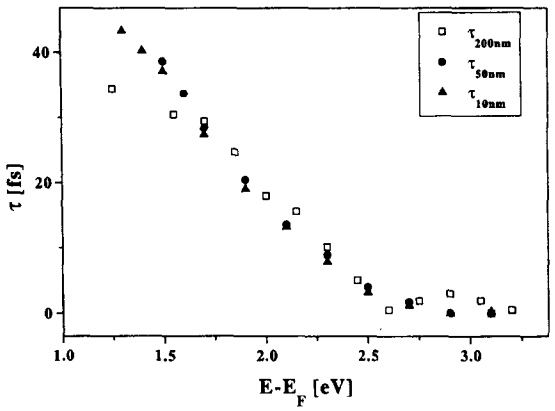

Fig. 9. Lifetime τ_{ps} obtained from measurements of polycrystalline gold films of different thickness. The film thicknesses are: 2000 Å (□), 500 Å (●), and 100 Å (▲).

The transport effect may also be reduced by using films as thin as the penetration depth of the laser light. Fig. 9 shows $\tau(\varepsilon)$ of three different gold films: 100, 500, and 2000 Å thick, respectively. The 100 and 500 Å were deposited on a BaF_2 crystal by conventional resistive evaporation technique (evaporator chamber preasure 10^{-6} mbar). The film thickness was determined by a crystal thickness monitor. Because the films have been exposed to air, the Auger spectra indicate some carbon contamination. This might explain the much lower work function and hence the wide energetic spectrum (1.3 eV $< \varepsilon <$ 3.3 eV). We checked the surface flatness of both films by means of scanning tunneling microscopy (STM) and found a rough surface, mainly colloidal grown features (grains size about 20 nm). This has to be expected because we were not able to heat the substrate during the film growing process. The 2000 Å thick gold film was also fabricated by evaporation; however, we used mica as a substrate. This film went through several heating and annealing cycles until the STM images shows a fairly smooth surface. The image shows hexagonal faceting (lines which meet at an angle of 120°) which is characteristic of the (111) closed-packed plane for Au. We

decreased the work function of the 2000 Å film slightly by depositing a small amount of Cs on the surface. This allow to expand the probed spectrum in order to check the leveling off effect due to transport. At higher energies ($\varepsilon > 1.8$ eV), where transport effect do not play a dominant role, the electron lifetimes τ(measured) observed for all three films are remarkably equal, taken into account the differences in thickness and surface roughness and that they were grown in different laboratories. At energies below 1.75 eV, the thicker film starts – in comparison to the two thinner ones – to level off. This might prove the expectation, that electron transport can be impeded by using thin films where the leaving electrons will be scattered back from the insulator–metal interface to the surface. However we did not find a difference in τ for the 100 and 500 Å thick films, what is in contrast with this interpretation. Further work is in progress with the aim of preparing atomically smooth, freestanding thin metal films. This allows the observation of intrinsic hot electron relaxation times without being affected by transport and inelastic scattering on the metal–insulator interface.

9. Concluding remarks

The present work shows that time resolved two-photon photoemission, based on the equal pulse correlation technique, can be used to investigate the competing channels for hot electron transfers. This technique provides a powerful tool for the systematic study of the dynamics of electron–electron scattering processes in noble and transition metals in the low density limit. While the inelastic lifetime T_1 of Ag is in qualitative and quantitative agreement with the Fermi liquid theory, the result obtained for Au is very different. Hot electron relaxation observations of metals with unoccupied d shells prove that the inelastic decay depends on the number of unoccupied d orbitals below the probed energy state. The observations reveal that copper is an ideal model substrate for studying the mechanism of hot electron charge transfer and the resonance lifetime τ_R. The rate for hot carrier transfer, however, might be quite different for the noble metal Cu and the more catalytic active transition metals due to a much faster decay of the excited electrons. We discussed the nature of polarization effects observed in our experiments. Differences in the observed lifetimes between parallel- and crosspolarized beams indicate that coherence effects have to be taken into account in this time scale. We have shown that the transport effect is a second competing channel for hot electron transfer. The effect might be minimized by using polycrystalline samples with small grains or thin films in the order of the optical penetration depth of the laser light.

Acknowledgements

The authors would like to thank C.A. Schmuttenmaer and M. Wolf for many helpful discussions. Financial support by the Swiss National Science Foundation is gratefully acknowledged.

References

[1] R.R. Cavanagh, D.S. King, J.C. Stephenson and T.F. Heinz, J. Phys. Chem. 97 (1993) 786.
[2] J.W. Gadzuk, L.J. Richter, S.A. Buntin, D.S. King and R.R. Cavanagh, Surface Sci. 235 (1990) 317.
[3] S.M. Harris, S. Holloway and G.R. Darling, J. Chem. Phys. 102 (1995) 8235.
[4] J.A. Misewich, T.F. Heinz and D.M. Newns, Phys. Rev. Letters 68 (1992) 3737.
[5] C.A. Schmuttenmaer, M. Aeschlimann, H.E. Elsayed-Ali, R.J.D. Miller, D.A. Mantell, J. Cao and Y. Gao, NSF Center for Photoinduced Charge Transfer, University of Rochester, unpublished results.
[6] C.A. Schmuttenmaer, M. Aeschlimann, H.E. Elsayed-Ali, R.J.D. Miller, D.A. Mantell, J. Cao and Y. Gao, Phys. Rev. B 50 (1994) 8957.
[7] E. Knoesel, T. Hertel, M. Wolf and G. Ertl, Chem. Phys. Letters (in press).
[8] P.J. Rous, Phys. Rev. Letters 74 (1995) 1835; Surface Sci. 326 (1995) 67.
[9] V. Dose, Surface Sci. Rep. 5 (1985) 337.
[10] K. Giesen, F. Hage, F.J. Himpsel, H.J. Riess and W. Steinmann, Phys. Rev. Letters 55 (1985) 300.
[11] D.F. Padowitz, W.R. Merry, R.E. Jordan and C.B. Harris, Phys. Rev. Letters 69 (1992) 3583;T. Hertel, E. Knoesel, E. Hasselbrink, M. Wolf and G. Ertl, Surface Sci. 317 (1994) L1147.
[12] J.J. Quinn, Phys.Rev 126 (1962) 1453.
[13] M. van Exter and A. Lagendijk, Phys. Rev. Letters 60 (1988) 49;R.H.M. Groeneveld, R. Sprik and A. Lagendijk, Phys. Rev. Letters 64 (1990) 784.

[14] M. Aeschlimann, S.Pawlik and M. Bauer, to be published.
[15] T.F. Heinz, S.L. Palfrey and K.B. Eisenthal, Opt. Letters 8 (1984) 359.
[16] A.J. Taylor, D.J. Erskine and C.L. Tang, J. Opt. Soc. Am. B 2 (1985) 663;S.L. Palfrey and T.F. Heinz, J. Opt. Soc. Am. B 2 (1985) 674.
[17] N.V. Smith, P. Thiry and Y. Petroff, Phys. Rev. B 47 (1993) 15476.
[18] S.D. Kevan, Phys. Rev. Letters 50 (1983) 526.
[19] R. Haight, J. Bokor, J. Stark, R.H. Storz, R.R. Freeman and P.H. Bucksbaum, Phys. Rev. Letters 54 (1985) 1302;C.H. Yang, J.M. Carlson-Swindle, S.A. Lyon and J.M. Worlock, Phys. Rev. Letters 55 (1985) 2359;L. Rota, P. Lugli, T. Elsaesser and J. Sahah, Phys. Rev. B 47 (1993) 4226;T. Kuhn and F. Rossi, Phys. Rev. B 46 (1992) 7496.
[20] W.S. Fann, R. Storz, H.W. Tom and J. Bokor, Phys. Rev. B 46 (1992) 13592.
[21] R.H.M. Groeneveld, R. Sprik and A. Lagendijk, Phys. Rev. B 45 (1992) 5079.
[22] H.E. Elsayed-Ali, T.B. Norris, M.A. Pessot and G.A. Mourou, Phys. Rev. Letters 58 (1987) 1212;R.W. Schoenlein, W.Z. Lin, J.G. Fujimoto and G.L. Eesley, Phys. Rev. Letters 58 (1987) 1680.
[23] H.E. Elsayed-Ali, T. Juhasz, G.O. Smith and W.E. Bron, Phys. Rev. B 43 (1991) 4488.
[24] M.P. Seah and W.A. Dench, Surface Interface Anal. 1 (1979) 2.
[25] G. Schönhense and H.C. Siegmann, Ann. Physik 2 (1993) 465.
[26] N.W. Ashcroft and N.D. Mermin, Solid state physics (Holt, Rinehart und Winston, New York, 1976).
[27] H.E. Elsayed-Ali and T. Juhasz, Phys. Rev. B 47 (1993) 13599.
[28] G. Chiarotti, ed., Physics of solid surfaces, Landolt-Börnstein Vol. 24b (Springer, Berlin).
[29] S.D. Brorson, J.G. Fujimoto and E.P. Ippen, Phys. Rev. Letters 59 (1987) 1962.
[30] C.A. Schmuttenmaer, M. Aeschlimann, J.W. Herman, R.J.D. Miller, D.A. Mantell, J. Cao and Y.Gao, Proc. SPIE 2125 (1994) 98.